

BACTERIORHODOPSIN

Janos K. Lanyi

Department of Physiology & Biophysics, University of California, Irvine, CA 92697-4560

1. INTRODUCTION

Bacteriorhodopsin (BR), a retinal protein in the cell membranes of extremely halophilic archaea, is the simplest known biological energy-conversion device. In this small (26 kDa) integral membrane protein, the reaction cycle in which the retinal is thermally reconverted from the photoproduct 13-*cis*,15-*anti* to the initial all-*trans* (the “photocycle”), drives the electrogenic translocation of a proton from the cytoplasmic to the extracellular side of the membrane (for reviews, see Mathies et al. 1991; Ebrey, 1993; Lanyi, 1993; Haupts et al. 1999; Lanyi, 2000a,b). The electrochemical gradient of protons created across the membrane is utilized for ATP synthesis and the secondary transport of amino acids and ions, as in many other prokaryotic cells and in mitochondria and chloroplasts. Thus, bacteriorhodopsin offers the organisms an alternative to the respiratory chain, of importance when the oxygen (at low concentration to begin with because of its poor solubility in its hypersaline, i.e. >20% NaCl, environment) is used up in a dense culture.

Most of the very large amount of work on bacteriorhodopsin over the past three decades has had the rationale to describe its transport function in relation to its structure. The first crystallographic determination of the structure of this protein (Henderson and Unwin, 1975) was from the extended 2-dimensional hexagonal arrays it forms *in vivo*, that contain specific lipids and bacteriorhodopsin as the only protein, the “purple membrane.” More recently, the unexpected ease of growing well-diffracting 3-dimensional crystals (Rummel et al. 1998), made it possible to obtain high-resolution structures for both the unilluminated state and some of the photointermediates of the transport cycle. There were technical advantages for describing the reactions of the retinal and the protein, not available in other systems, in attempts to understand the mechanism of the transport. Analysis of photostationary states, particularly at cryogenic temperatures, provided much information about the intermediate states of the cycle. Time-resolved spectroscopy was made possible by triggering single turn-overs of the cycle with nanosec or shorter laser pulses, and the development of a large variety of spectroscopic methods for measuring the transient changes in real time. The spectroscopic methods available include optical measurements in the UV-visible range (Lanyi and Váró, 1995), FTIR (Maeda, 1985) and resonance Raman spectroscopy (Althaus et al. 1995), NMR (Zheng and Herzfeld, 1992), and ESR (Steinhoff et al. 1994; Thorgeirsson et al. 1994; Pfeiffer et al. 1999) measurements with covalently linked spin labels. Such experiments have been done with hundreds of site specific mutants, which defined the residues of functional and structural importance. The outcome of these studies is a step-by-step mechanism for the proton transport and how it is driven by the isomerization of the retinal. Although controversies continue to abound in the bacteriorhodopsin field,

and the models are numerous and still evolve, strong hints have emerged as to the principles that underlie active transport in this protein and probably in other pumps as well.

2. STRUCTURE

Although it is not a signal receptor, bacteriorhodopsin has been regarded as the prototype of the structure of G-protein linked receptors. First cryo-electron microscopy of 2-dimensional crystals to 3 Å resolution (Henderson et al. 1990; Grigorieff et al. 1996; Kimura et al. 1997), and more recently X-ray diffraction of 3-dimensional crystals to 1.9 (Belrhali et al. 1999) and then 1.55 (Luecke et al. 1999) Å resolution, yielded a very detailed structure for this integral membrane protein. Most of the 248 amino acid residues in the single polypeptide chain are arranged in seven transmembrane helices labeled A through G. Sequence comparisons among bacteriorhodopsins (and other bacterial rhodopsins with different physiological functions) from various sources, mutation and deletion analysis, and proteolytic digestion studies have revealed that the short extramembrane segments, including the extracellular N-terminus and the cytoplasmic C-terminal tail, have little or no functional or structural role. Neither does the trimeric arrangement of the protein in the hexagonal lattice have a functional significance, as the monomer is competent in transporting protons (Dencher and Heyn, 1979). The functional parts of bacteriorhodopsin are therefore to be found in the intramembrane portion of the seven-helical structure.

Helices E, F, and G are approximately perpendicular to the plane of the membrane, while A, B, C, and D traverse the membrane with tilts at small angles from the normal (Figure 1). Together, the seven helices enclose a cavity that spans the width of the membrane, filled with amino acid side chains and the transversely lying retinal. This cavity defines the pathway of the proton during its transport across the membrane. The retinal is linked to the ϵ -amino group of Lys-216, near the middle of helix G, and forms a positively charged protonated Schiff base. Because of interaction of the retinal with neighboring charges in the binding pocket, particularly with the anionic Asp-85 and Asp-212, and the planarity of the polyene chain and ionone ring of the retinal, the maximum of the broad absorption band of the chromophore is considerably red-shifted from model compounds, to 568 nm for the all-trans isomer (hence the name, "purple membrane"). The Schiff base divides the cavity into two sections usually (and inaccurately) called extracellular and cytoplasmic half-channels. These are occluded pathways rather than open pores, and the term "channel" is meant to indicate only that these regions do, at some time during the transport cycle, conduct protons or perhaps hydroxyl ions. The extracellular region contains numerous charged and polar residues with functional roles. The most important of these is the anionic Asp-85, the main component of the counter-ion to the Schiff base and the proton acceptor when the Schiff base becomes deprotonated during transport. Other residues of interest are Asp-212, Arg-82, Glu-204, and Glu-194, with roles in proton release to the extracellular surface during the transport. The cytoplasmic region, in contrast, contains mostly hydrophobic residues, with the important exception of the protonated Asp-96 that is the proton donor to the Schiff base late in the photocycle. The transport is remarkably independent of any one residue.

It is affected by many single mutations, but completely abolished only when Lys-216 or Asp-85 are replaced (although there are exceptions even to this rule).

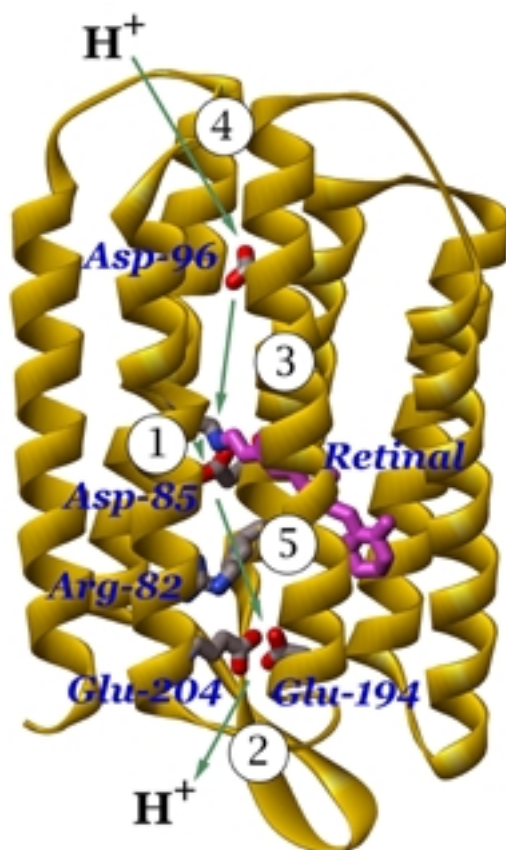


Figure 1. An overview of the seven-helical structure of bacteriorhodopsin. The all-trans retinal is shown in purple, important residues in blue. The path of proton translocation is shown with green arrows. Protonation/deprotonation steps follow one another as numbered: *step 1* is protonation of Asp-85 by the Schiff base, *step 2* is proton release to the medium, *step 3* is reprotonation of the Schiff base by Asp-96, *step 4* is reprotonation of Asp-96, and *step 5* is proton transfer from Asp-85 to the proton release group. (Reproduced with permission from Luecke et al. Science 286, 255-260, 1999. Copyright 1999 American Association for the Advancement of Science).

The active site is centered around the highly polarized water 402 (Luecke et al. 1998), which donates hydrogen-bonds to Asp-85 and Asp-212, and receives one from the protonated Schiff base. Figure 2 shows the electron density map of this region at 1.55 Å resolution.

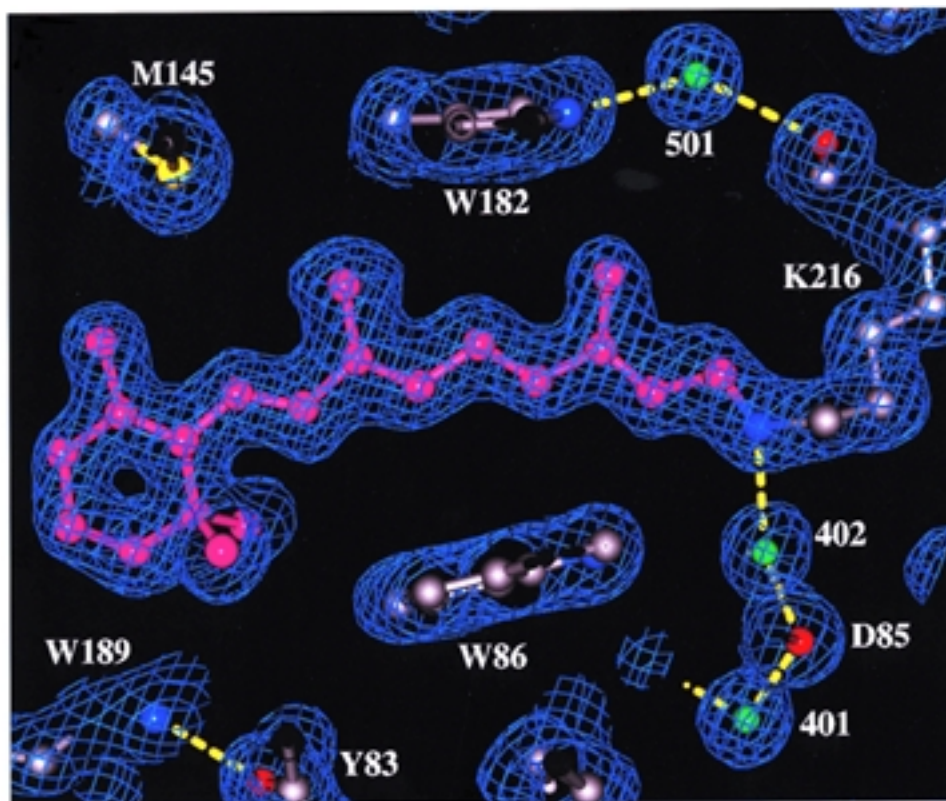


Figure 2. Electron density map of the Schiff base region. It shows the all-trans retinal, water 402 that bridges the Schiff base and Asp-85 and is connected to water 401, water 501 that connects helix G with helix F, and two tryptophan side-chains that sandwich the retinal polyene chain. (Reproduced with permission from Luecke et al. *J.Mol.Biol.* 291, 899-911, 1999).

Burying the three charged groups has an energy cost, which is compensated by the free energy gain when forming an extended array of hydrogen-bonds around water 402, dependent on the negative charge of Asp-85. Immediately near the Schiff base region, Asp-85 is hydrogen-bonded to Thr-89, as well as to water 401, while Asp-212 is hydrogen-bonded to water 406, Tyr-57 and Tyr-185. A 3-dimensional hydrogen-bonded network of side-chains and four additional water molecules leads from water 406 and Tyr-57 to the extracellular surface (Belrhali et al. 1999; Luecke et al. 1999).

There are much fewer bound water molecules on the cytoplasmic side. Water molecules 501 and 502 are both located near the middle of helix G, hydrogen-bonded to the C=O of Ala-215 and Lys-216, respectively (Luecke et al. 1999a). Water 501 is hydrogen-bonded additionally to the indole ring of Trp-182 on helix F, thereby bridging helices F and G. The hydrogen-bonds at helix G distort the otherwise α -helical structure, and result in a short π -helical run, a “ π -bulge.” This is a kink, with α -helical segments on either side, that introduces a change of direction in the middle of helix G. The ir-

regularity in the otherwise rigid helix makes it possible to change the spatial relationship of helices F and G, as indeed occurs after the retinal is photoisomerized. There are few other polar groups in this region, and the environment of Asp-96 near the cytoplasmic surface lacks polar side-chains and water. This, and a hydrogen-bond between its COOH group and the side-chain of Thr-46 account for the extraordinarily high pK_a of this aspartic acid.

There is a great deal of additional, less direct evidence for the presence of specifically bound water near the Schiff base. FTIR difference spectra in the region of O - H stretch had revealed changes in the hydrogen bonding of water molecules in various photointermediates (Maeda, 1995; Maeda et al. 1997). The positive and negative O - H stretch bands from these waters, from the photoproduct and the depleted BR state, respectively, are either shifted or absent in mutants of amino acid residues near the Schiff base and the extracellular or the cytoplasmic regions, providing clues to their locations, and suggest structural or functional roles for bound water in proton transfer. Consistent with this idea are well-defined changes in the photocycle when water is withdrawn from the protein, either at lowered humidity or by osmotic agents. At moderate dehydration, when the binding of water at the surface is decreased, the main effect is to inhibit proton transfer from Asp-96 to the Schiff base (Cao et al. 1991). Consistent with this, the structural changes proposed to lower the pK of Asp-96 through increased binding of water at the cytoplasmic surface are blocked at decreased hydration (Sass et al. 1997; Kamikubo et al. 1997).

The retinal polyene chain is immobilized by aromatic residues that surround it. In the region proximal to the Schiff base, Trp-86 and Trp-182 make contact, and in the distal region Trp-138 and Trp-189. Steric interaction between the 13-methyl group of the retinal with residue Trp-182, and the 9-methyl (as well as the 13-methyl) with Leu-93, have been deduced from the changed photocycles upon replacing or removing either the residues (Delaney et al. 1995; Yamazaki et al. 1995; Weidlich et al. 1996) or the methyl side chains in question. In the crystallographic structure, the potential steric conflict between the 13-methyl retinal group and the indole ring of Trp-182 is particularly evident. Thus, the retinal binding pocket appears to be rather rigid. Since the misfit of the photoisomerized retinal in its binding site must be one of the driving forces of the thermal reactions in the photocycle, the question of the compliance of the binding pocket in accommodating a change from a linear to a bent polyene chain is of obvious mechanistic and energetic importance.

3. THE PHOTOCYCLE

3.1 Transient spectroscopy

The need to measure the absorption changes of the bacteriorhodopsin chromophore in real time after laser pulse photoexcitation was a strong impetus for developing instrumentation for transient spectroscopy and methods to analyze the complex data generated. In the visible range, two kinds of transient spectroscopy have been used: sin-

gle wavelength time-course measurements, and optical multichannel spectral measurements. Both begin with photoexcitation of the sample with a short (typically a few nanosec) laser pulse. The quantum yield for photoisomerization and the spectral overlap between the initial state and the K intermediate limit the maximum extent of photoconversion to about 45%. In practice, the flash intensity is usually set to much less than saturating to avoid double-photon events and photodestruction of the chromophore, and the photoconversion does not exceed 15-20%. This means that all changes originate from a small fraction of bacteriorhodopsin, and the spectra measured are difference spectra. To reconstruct the spectra of the photoproducts one must know, or correctly estimate, the fraction of bacteriorhodopsin that cycles.

Following absorption changes at single wavelengths yields traces for the time-courses with typically very high signal/noise ratio. Often the data are collected at evenly spaced time-intervals after the flash excitation, but processed to reductively average the collected points over time and yield a logarithmic time-scale. Rich in information in the time-domain, such data are used to determine the relaxation time-constants. Inclusion of data from several wavelengths in the analysis, so as to include large-amplitude changes from all intermediates, generates more reliable, global time-constants. The bacteriorhodopsin photocycle can be described with up to 6-7 time-constants. In simple systems the time-constants, or at least some of the time-constants, might be equivalent to the reciprocals of the rate constants, but this is unlikely for a complex reaction sequence like the bacteriorhodopsin photocycle. Although the analysis of the data will also produce a set of difference spectra associated with the time-constants, the wavelengths of the measurement have to be numerous and closely spaced if these are to be of use. Even when well-defined, these spectra usually represent mixtures of intermediates from reactions that overlap in time.

Optical multichannel measurements use linear diode or charge-coupled device (CCD) arrays to produce entire difference spectra at specified time-delays after the flash. The spectrum from a grating placed after the sample is projected onto the photosensing array, made responsive with a high-voltage pulse during the desired time-window after the flash, and generates a set of intensities in many, at least several hundred, channels. Data are collected with and without a flash, and averaged extensively to increase the inherently poor signal/noise ratio. The calculation from a data set yields a difference spectrum for a single time-point, and the measurement is repeated for as many time-points as desired. Typically, multichannel experiments are rich in spectral information. Their combination with single wavelength measurements overcomes the limitations of either method.

The information one would want to glean from these measurements are the spectra of the intermediate states, the time-courses of their rise and decay, and a kinetic scheme with rate-constants which account for all the data. If all these were produced, one would have "solved" the photocycle. Unfortunately, the number of observable parameters in the data are fewer than what is needed to determine the number of unknowns. Attempts to produce a solution use additional assumptions, for example about the temperature-dependencies of the calculated rate constants or the shape of the cal-

culated spectra. Even with such assumptions, an exact solution has not been found. There are always small but persistent deviations from the predictions of simple kinetic models. Nevertheless, approximate solutions have been useful. They have raised, even if not proved, the possibilities of reversible (as opposed to irreversible) reactions in the cycle, and placed limitations on branches and cul-de-sacs, or the existence of multiple states with separate photocycles.

Although arguments still rage about how to find the photocycle scheme that would be in full accord with the data, maybe it is futile to expect that there is one. It is possible that in a system with as many degrees of freedom as in a protein, the observable reactions can never be described by schemes as simple as one is used to in the kinetics of small molecules. For example, an ensemble of protein conformations might result in an ensemble of activation barriers to a single photocycle reaction. In that case, the reaction will be not quite exponential and not fully amenable to conventional kinetic analysis. Analyses with such “distributed” kinetics do produce exact fits, but only at the expense of additional and unproved assumptions.

3.2 Steps of the photochemical cycle

Absorption of light by the all-*trans* retinal chromophore causes isomerization to 13-*cis*,15-*anti*. Since in this configuration the C₁₃-C₁₄ double bond, but not the C₁₅-N double bond, has rotated, maintaining normal bond angles requires that the polyene chain assume a sharply bent shape. One would expect this will be opposed by constraints of the retinal binding pocket, and lead to an initially strained retinal configuration. If the retinal is replaced with an analogue with a ring to bridge the C₁₃-C₁₄ bond, so as to immobilize it in the *trans* configuration, the initial state of the chromophore is very rapidly (in nanosec) recovered. Otherwise, the photoisomerized retinal relaxes, and then re-isomerizes to all-*trans*, on a much slower time-scale (tens of msec) and through a series of intermediate states in which either the retinal or the protein, or both, have detectable differences from the initial state (reviewed in Lanyi and Váró, 1995). This process, termed the “photocycle” even though only its first step is dependent on light, is equivalent to the reaction cycles of enzymes and transport or signaling proteins. Much effort has been expended on understanding its details with respect to the underlying driving force of proton transport (bond rotations of the retinal), the pathway and directionality of proton transport (protonation state of residues, and why they change their pK_as), and the energetics (kinetics, and the exchange of excess free energy in the interconversions of intermediate states).

A schematic representation of the photocycle is given in Figure 3. The K intermediate, that rises in a few nsec after absorption of a photon, contains a distorted, *i.e.*, twisted, 13-*cis* retinal. Although the exact nature of this twist is not yet clear, it must be near the C₁₃-C₁₄ double bond where the isomerization had taken place, *i.e.*, near the Schiff base. K is the first well-defined intermediate state, and the photocycle can be considered as its relaxation, driven by the excess enthalpy (about 50 kJ/mol) that remains after decay of the excited state. The red-shifted K state converts to the blue-shifted L intermediate in about 1 μsec. In the L state the displacement of the Schiff base relative to

Asp-85 results in local reorganization of the protein. In the unilluminated BR state, the Schiff base titrates with a very high pK_a (> 11), and Asp-85 with a very low one (about 2.5). Because of the changed geometry at the Schiff base in L, the pK_a difference between the proton donor Schiff base and the proton acceptor Asp-85 is greatly decreased. The new protonation equilibrium that develops, in about 10 μsec , no longer favors the Schiff base as completely. The Schiff base thereby loses its proton while Asp-85 becomes protonated.

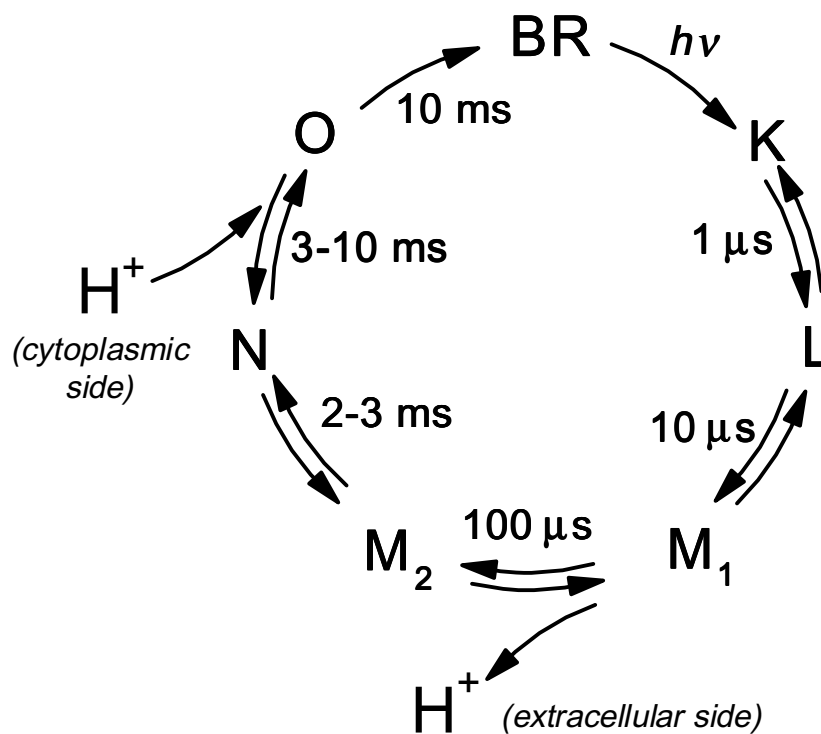


Figure 3. Intermediates of the bacteriorhodopsin photocycle, with the approximate relaxation times of the reactions at room temperature. In the K state the retinal is already photoisomerized from all-trans to 13-cis,15-anti. The retinal and its binding site are somewhat relaxed in the L state, and the pK_a s of the retinal Schiff base and Asp-85 decrease and increase, respectively. The first protonation equilibrium, of L with the M₁ state still contains much protonated Schiff base, but in the second, of M₁ with M₂, the Schiff base will have been completely deprotonated. The Schiff base comes to a new protonation equilibrium, with Asp-96, in the M₂ to N reaction, and Asp-96 is reprotonated and the retinal is reisomerized in the N to O reaction. Recovery of the initial BR state from the O intermediate, with protonated Asp-85 and a twisted retinal, is strongly unidirectional.

The bacteriorhodopsin intermediate with deprotonated Schiff base is easily detected through its strongly blue-shifted absorption maximum (near 400 nm), and its

various forms are referred to as the M states. The time-course of the formation of M is complex. Fits to multiexponential kinetics detected 3 or 4 rise components. Some of this complication could reflect the presence of back-reactions, i.e., the development of equilibrium mixtures with successively increasing amounts of the species with deprotonated Schiff base. This would imply that other things happen in the protein along with the deprotonation of the Schiff base. The M state produced first, that is in equilibrium with L, was termed M_1 . In about 100 μsec , M_1 produces a second M, that has, under some conditions a blue-shifted absorption maximum, and termed the M_2 state (Zimányi and Lanyi, 1992b).

The existence of an equilibrium is usually tested by following the relaxation process after a perturbation. In the bacteriorhodopsin photocycle this can be accomplished with a second flash to rapidly deplete, for example, the M state. If the photocycle kinetics after the second flash proceed unchanged, although with lowered amplitude, there is no reason to conclude the existence of an equilibrium. If M recovers partly at the expense of another intermediate state, and with kinetics that resemble the interconversion of that state with M, the existence of an equilibrium is formally proved. Such experiments, with the D96N mutant where the M to N reaction is very slow, supported the interpretation of the M kinetics as successive equilibria between L and two M states (Brown et al. 1998b).

It is likely, however, that this model with two M states is oversimplification. Two M states are neither sufficient to account for all that happens in the protein after deprotonation of the Schiff base but before its reprotonation (conformational changes of side-chains and the retinal, rearrangements of water, proton release to the surface, etc.), nor can they fully explain the complex kinetics.

Decay of the M state is also complex, and suggest the rise of successive equilibria that contain decreasing amounts of M. First, M_2 comes to an equilibrium with the next state in the photocycle, the N intermediate, in a few msec. In the N intermediate the Schiff base is protonated, but the isomeric state is still 13-*cis*. As the $L \leftrightarrow M$ equilibrium, the $M \leftrightarrow N$ equilibrium is also supported two-flash experiments (Druckmann et al. 1992). The Schiff base reprotonation is independent of pH, as the proton donor is internal, the initially protonated Asp-96. At $\text{pH} > 8$ the rates of the reactions are poised so as to delay the decay of N relative to the decay of M, and under these conditions the ratio of N to M is revealed to be about 5:1. This implies that at this time in the photocycle the difference in the pK_a of the proton donor Asp-96 and the acceptor retinal Schiff base is only about 0.7 pH units. The protonation equilibrium between the Schiff base and Asp-96, i.e., the $M_2 \leftrightarrow N$ equilibrium, is shifted toward more complete transfer of the proton to the Schiff base as Asp-96 gains a proton from the cytoplasmic surface and then the retinal reisomerizes to all-*trans* in the strongly red-shifted O intermediate. As the new equilibrium of M with N and O is attained there will be a second decay component for M. Unlike the first, the second decay phase of M is pH dependent, most noticeable at $\text{pH} > 8$ where the protonation of Asp-96 limits the N to O transition. Thus, the decay of N, and therefore M, becomes slower with increasing pH.

The idea of an equilibrium between the N and O states is supported by a perturbation experiment similar to those used to study the L to M, and the M to N reactions but one that used a temperature jump (Chernavskii et al. 1989). This equilibrium is pH dependent, and at lower pH it is mostly O that accumulates. The apparent pK_a is about 7. Because in the N state Asp-96 is unprotonated (under most conditions) but in O it is protonated, it seems that the pK_a refers to the reprotonation of Asp-96. There is evidence that protonation of Asp-96 is a prerequisite to the rapid reisomerization of the retinal to all-trans.

In the O state the retinal is in a twisted all-trans configuration, and Asp-85 is still protonated. In the last step the O intermediate regenerates the initial bacteriorhodopsin state in a virtually irreversible reaction. The rate of O decay is determined by how rapidly the proton of Asp-85 is lost (Richter et al. 1996a). Thus, the large loss of free energy (that makes this a unidirectional reaction) originates from the recovery of the initial low pK_a (2.5) of Asp-85. At physiological pH this makes the deprotonation of Asp-85, and therefore the decay of O, a strongly downhill reaction.

To summarize, from close examination of the photocycle it appears that the Schiff base of the photoisomerized retinal mediates, in effect, the transfer of a proton from Asp-96 on the cytoplasmic side to Asp-85 on the extracellular side. This occurs by a multi-step process that is understood in molecular terms. However, in a mathematical sense the kinetics of the interconversions of the intermediates in the photocycle are still not fully solved. It has been argued that the multiphasic decay and rise times for most intermediates could be caused equally well by heterogeneity of the initial state and a separate photocycle from each population. In the absence of convincing evidence for such complications, and evidence that supports the idea of transient equilibria between successive intermediates, there is tentative agreement that at least some of the kinetic complexities originate from the presence of reversible reactions in a single photocycle. In such models, equilibria arise because the forward and reverse rates are not greatly different. This means that the free energy changes in the internal proton exchange reactions are small, and the pK_a s of the proton donors and acceptors are well-matched (Váró and Lanyi 1991).

3.3 Proton transfer events near the membrane surfaces

The net displacement of a proton from the cytoplasmic to the extracellular side of the retinal Schiff base results in additional proton transfers near the surfaces, and between the two membrane surfaces and the bulk solution.

The first of these events is that protonation of Asp-85 causes the release of a proton to the extracellular surface. The existence of mutual interaction between the protonation states of Asp-85 and the more peripherally located Glu-194/Glu-204 region is indicated by the observation that there are two apparent pK_a s when Asp-85 is titrated (Balashov et al. 1996), as shown in Figure 4.

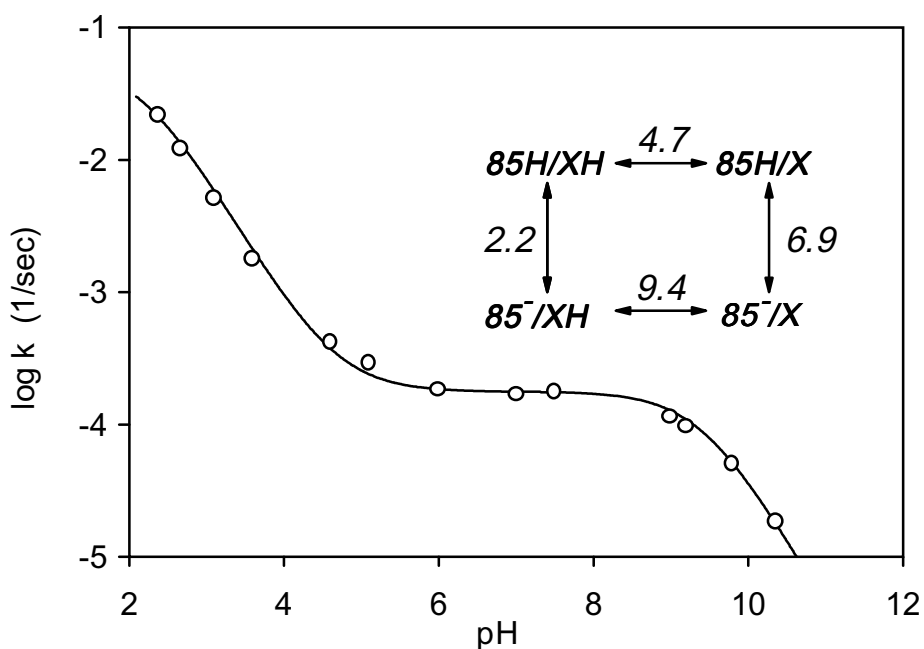


Figure 4. pH dependence of the rate of retinal isomeric equilibration, that is equivalent to titration of Asp-85. The two pK_a s observed suggest the model of Balashov et al. 1996 in which the dissociation of Asp-85 is coupled to the dissociation of group XH (inset). (Redrawn from Richter et al. *Biochemistry* 35: 4054-4062, 1996).

Such titrations are performed in the dark, and are based on a shift of the chromophore band to longer wavelength (a purple to blue color shift) when the protonation of Asp-85 removes its negative charge near the retinal Schiff base. Alternatively, they are based on the rate of the thermal equilibration between the all-trans and 13-cis,15-syn retinal isomeric states, dependent on the protonation state of Asp-85. The finding of two apparent pK_a s is accounted for by a model (Figure 4, inset) in which the pK_a of Asp-85 is raised when another proton-binding site is deprotonated, and likewise the pK_a of the site is raised when Asp-85 is deprotonated. Thus, at neutral pH either Asp-85 or the site is protonated but not both. The anomaly of the titration is absent (Richter et al. 1996b) when Glu-194 or Glu-204 is replaced with a non-protonable residue, such as Gln, and when Arg-82 is replaced by Gln or Ala. Significantly, these are the same mutations that eliminate release of a proton during the rise of M. Although such titrations are with the retinal in the all-trans state, the coupling they reveal explains therefore the events that follow protonation of Asp-85 in the photocycle.

In the M state, after the initially anionic Asp-85 becomes protonated, the positively charged side-chain of Arg-82 swings away from it and toward the Glu-194/Glu-204 pair near the extracellular surface (Luecke et al. 1999b). The displacement of the positive charge along the membrane normal is 1.6 Å. The reason might be simply the loss of the negative charge of Asp-85, but probably also the hydrogen-bonding of water 401 to Asp-212 instead of water 406. Before illumination, water 406, through water 401, connects Asp-85 to Arg-82, but it is not evident in the structure of M. Instead of hydrogen-bonding with water 406, Arg-82 forms a new hydrogen-bond with water 405, which

now interacts with Glu-194 and Tyr-83 as well (Figure 5). The shuttling of the Arg-82 side chain between the “up” and “down” orientations thus appears to be the means for coupling the pK_as of Asp-85 and the proton release site.

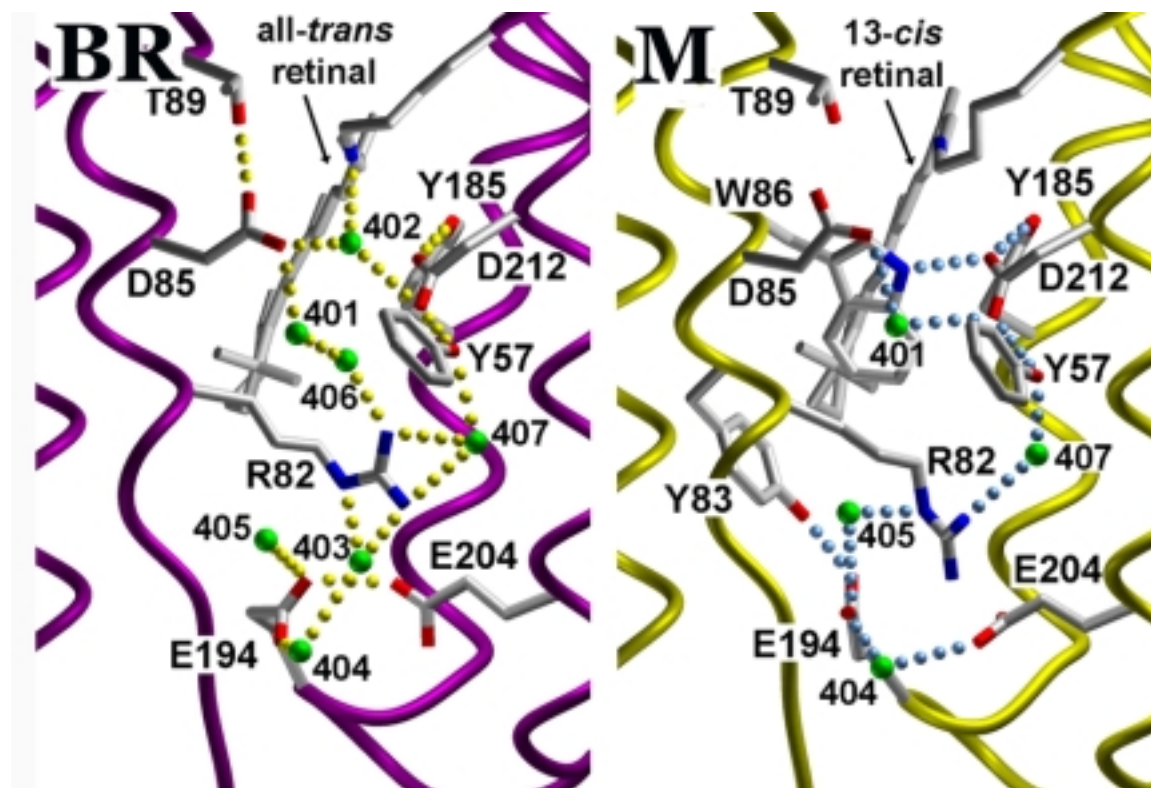


Figure 5. Comparison of the extracellular region in unilluminated bacteriorhodopsin (A) and in the M intermediate of the D96N mutant (B). Note the disruption of the hydrogen-bonded chain of side-chains and water molecules in M, and the approach of the guanidinium group of Arg82 toward the Glu-194/Glu-204 pair. (Reprinted with permission from Luecke et al. *J.Mol.Biol.* 291, 899-911, 1999).

However, the origin of the released proton has not yet been identified. The suggestions that the proton is from Glu-204, or that it is a proton shared by Glu-194 and Glu-204, are contradicted by the absence of the negative C=O stretch band expected from depletion of a protonated COOH (Rammelsberg et al. 1998). One of the several water molecules in this region (by dissociation of either H₂O or H₃O⁺), or the hydrogen-bonded network (containing a delocalized proton), seem to be better alternatives. The latter is suggested by the observation of the decrease of a broad continuum infrared band (Rammelsberg et al. 1998), correlated in time and in mutants with the release of a proton in the photocycle.

The released proton can be detected in real time by following the absorption changes of a pH indicator dye (Heberle and Dencher, 1992), either covalently linked to a

surface residue on the extracellular side (to Lys-129 or an engineered cysteine since bacteriorhodopsin does not contain a cysteine) or added to the bulk solution. In the former case the time-constant for release is between 50 and 100 μ s, which is similar to the time-constant of the major phase of M rise. In the latter case, the appearance of the proton is later, with a time-constant of about 1 ms. The difference is attributed to the fact that the proton is carried by buffering groups, whose concentration is high at the membrane surface (protein residues and lipids), but lower in the bulk (dye molecules). Indeed, there is hardly any delay for the appearance of the released proton when the indicator dye is on the cytoplasmic surface, so that the proton has to move along the extracellular side of the membrane and cross to the other side before being detected (Heberle et al. 1994; Scherrer et al. 1994).

The absorption changes of the dyes reveal also proton uptake at the cytoplasmic surface during the decay of N. This proton will reprotonate Asp-96. The path of the proton from the bulk solution to the surface, and from surface to Asp-96, is not yet clear, however. Replacement of the four acidic residues on the cytoplasmic surface, Asp-36, Asp-38, Asp-102, and Asp-104, with Asn causes only minor (< 3-fold) change in the N kinetics (Brown et al. 1999). There is an about 10x slowing of M decay when Asp-38 is changed to an arginine, a conformational effect on the proton exchange between Asp-96 and the Schiff base (Riesle et al. 1996). In addition, few of the surface aspartic acids are conserved among different bacteriorhodopsins, and the D38R change is one of the naturally occurring variabilities. It appears, therefore, that capturing the proton at the surface, perhaps by a proposed “proton funnel” is not a rate-limiting step in the photocycle.

3.4 Infrared spectroscopy of the photointermediates

Vibrational spectroscopy has been a valuable tool in describing the events of the photocycle in molecular terms. Unlike spectra in the visible that contain a single broad band, vibrational spectra contain a wealth of bands, from both the retinal and the protein. Resonance Raman spectra provide information about C-C, C=C, C-H, C=N, and N-H bond changes in the retinal (Althaus et al. 1995). Infrared (Fourier Transform Infrared, FTIR) spectra contain bands from these, as well as from protonation of acidic residues and changes in hydrogen-bonds of protein groups and water (Maeda, 1995). Each of these methods has its advantages and disadvantages. With the resonance Raman method the vibrational modes of the desired intermediate can be selectively enhanced by providing excitation at wavelengths absorbed by the chromophore. However, time-resolution is not simple to achieve. It requires steady photoexcitation at a location physically removed from the measuring beam, and that after a time-delay the sample flow as a liquid, or rotate as a film, into the beam.

The infrared spectra of proteins are dominated by the C=O stretch and N-H rock of the numerous peptide bonds, the amide I and amide II bands. Changes that relate to function appear as small perturbations superimposed on this pattern. For this reason, FTIR spectra of the photocycle intermediates must be measured as difference spectra, in which the bands are positive for the photoproduct, and negative for the depleted initial state. The measurement time is much shorter than for Raman spectra, and the experi-

ment can be done after flash in real time with a stationary sample. In the “rapid-scan” mode, each flash is followed by repeated sampling over time, with complete forward and return movement of the interferometer mirror for each time-point. In the “step-scan” mode, data are collected after every flash over the time-domain of interest, but only at a single position of the mirror. For a complete data set, the interferograms for the time points are calculated from data collected at all mirror positions after advancing the interferometer mirror between flashes. Rapid-scan measurements use the flashes more efficiently, but have a time-resolution of ten to hundred millisecond. Step-scan measurements use more flashes (and often more time) to collect the same data, but the time-resolution can be as fast as a hundred nanosecond.

Producing photostationary states at cryogenic temperatures is another way to accumulate the intermediates of the photocycle, for study with resonance Raman and FTIR (as well as NMR) spectroscopy, as with spectroscopy in the visible region. While the extent of photoconversion is usually much higher, and thus the signal/noise ratio much improved, in this kind of experiment, one may question if the K, L, etc. intermediates produced at 100 K or 170K, for example, are the same states produced at ambient temperature during transport. Often, the details of FTIR spectra indicate, however, that the differences are minor.

Of the vibrational bands that originate from the retinal, the largest is from the ethylenic (C=C) stretch mode between 1505 and 1570 cm^{-1} . The frequency is related to the absorption maximum in the visible, making it useful for relating the vibrational spectra to those in the visible and thereby identifying what states, or mixtures of states, are present. The C-C single bond stretch frequencies between 1100 and 1300 cm^{-1} (fingerprint region) reveal whether the isomeric state of the retinal is all-*trans* (as in BR and the O state) or 13-*cis*. At lower frequencies, between 800 and 1,000 cm^{-1} , the hydrogen-out-of plane (HOOP) modes indicate twist of the retinal skeleton, great in the K and the O states but much diminished in the other states. Unfortunately, the amplitudes of all chromophore bands are much smaller when the Schiff base is unprotonated. Thus, FTIR spectra contain little information about the retinal in the M state.

The C = O stretch band of a protonated carboxyl group is between 1700 and 1760 cm^{-1} , depending on its state of hydrogen bonding. In the FTIR difference spectra for the L intermediate a broad negative band is seen at 1740 cm^{-1} that originates from perturbation of Asp-96 and Asp-115. The former is shifted to a somewhat higher frequency, and the latter to a lower frequency, as indicated by the FTIR spectra of the D115N and D96N mutants. Deprotonation of Asp-96 has been suggested to account for its negative band, but the proton from such a process has not been detected. Upon deprotonation of the Schiff base in the M state the appearance of a positive band at 1762 cm^{-1} indicates protonation of Asp-85. Although its frequency shifts to 1755 cm^{-1} once in the N state, this band persists in the O intermediate indicating that Asp-85 remains protonated until the end of the photocycle. Decay of the M state results in the appearance of a negative band at 1740 cm^{-1} that reflects deprotonation of Asp-96. The M, and particularly the N state, are characterized also by changes in the amide bands. The largest of these is a pair of

positive and negative bands at 1650 and 1670 cm^{-1} in N (Braiman et al. 1991). It is observed already in the M intermediate of the D96N mutant, termed the M_N state.

3.5 Crystallography of intermediate states

Two-dimensional crystals of bacteriorhodopsin have been utilized to advantage for studying structural changes in the photocycle. The purple membranes are solubilized with detergent, and larger arrays than occur *in vivo* are grown, through slow removal of the detergent. Cryo-electron microscopy of these sheets yields maps with the best resolutions at 3 Å. The images are usually projection maps, but from diffraction measured for tilted samples, 3-dimensional maps can be constructed as well. The maximal tilt being limited by technical problems, these maps tend to resolve features better in the membrane plane than along the membrane normal, and better at the center of the membrane than near its surfaces. The maps obtained in this way are usually difference maps, and so far have been able to indicate only very roughly that in M and N large-scale changes occur in the helices. Assignment of the density changes to an intermediate is indirect. One approach is to freeze the sample in liquid pentane after exposing it to a flash, and to correlate the time delay between flash and freezing with the kinetics of the various intermediates in membrane suspensions (Subramaniam et al. 1993). Another approach is to produce a photostationary state in a mutant where a photocycle step is sufficiently slowed to accumulate the intermediate of interest. In either case, the low occupancy of the intermediate is a problem. If the flash is short enough to produce a single-photon photocycle (nanosec), the fraction of bacteriorhodopsin that enters the photocycle is only 20-30%. In photostationary states only the intermediate M can be accumulated with 100% yield. Because all bacteriorhodopsin species are photoactive, and because the absorption spectra of all states but M overlap strongly with that of the unconverted state, it is not possible to convert more than 30-40% of bacteriorhodopsin to K, L, N or O. Usually, the amount is less. A low-resolution map for N was produced at 30% occupancy, from the photostationary state of the F219L mutant with greatly slowed N decay (Vonck, 2000). A third approach is to study mutants, which for various reasons seem to resemble photocycle intermediates. The projection map of the unilluminated D96G/F171C/F219L mutant resembles those of the M and N intermediates (Subramaniam and Henderson, 2000). This correlation was an unexpected finding in the triple mutant in which each of the three mutations slows the rates of reactions in the second half of the photocycle. The 3-dimensional map confirmed the tilt of helix F in the unilluminated protein.

X-ray diffraction of 3-dimensional crystals, grown with the cubic lipid phase method, has yielded maps with resolution as far as 1.55 Å (Luecke et al. 1999a), which is more than sufficient for identifying hydrogen bonds and the positions of bound water. Time-resolved crystallography, while in principle possible, has not been done successfully to date. Intermediates can be accumulated instead in photostationary states at various temperatures, with problems much the same as for cryo-electron microscopy. The structural changes in the K (Edman et al. 1999) and L (Royant et al. 2000) intermediates have been investigated by producing them by illumination at cryogenic temperatures (100 K and 170 K, respectively) in crystals, and calculating their electron density

maps. The difficulties of this approach not always appreciated (as argued in Balashov and Ebrey, 2001). The measured spectra will reveal, of course, what intermediate is produced and in what amount. The low occupancy of these states requires that the crystallographic resolution be unusually high so, as to fully define the structure of the minority state. The maps for M, where the photoconversion is nearly complete, are to date at resolutions of 2 Å or better, and these allow conclusions about the changed dispositions of side-chains and water. The quality of the maps suggest, however, that for refining structures with occupancy below 50% the resolution must be much better than 1.6 Å. Indeed, although FTIR spectra show distinct changes in the L state, very little structural change could be observed in a mixture of 40% L and 60% unconverted bacteriorhodopsin at 1.65 Å resolution (Luecke, Schobert, Cartailler, Lanyi, unpublished results). For these reasons, one must be cautious in making conclusions from such data.

The unilluminated D85S mutant was predicted to be an O-like state, from the analogy of the mutant to the O state as regards the isomeric state of the retinal and the charge state of residues 85 and 96 (Turner et al. 1993; Dioumaev et al. 1998). Indeed, small differences at the retinal Schiff base, i.e., the absence of a negative charge on residue 85 and loss of the hydrogen-bond between water 402 and Asp-212, result in large-scale helical tilts opposite to those observed in the M and N states (Rouhani-Manshadi, Cartailler, Faciotti, Walian, Needleman, Lanyi, Glaeser, Luecke, in preparation). Here, the outward tilts of several helices are on the extracellular, rather than the cytoplasmic, side.

4. MECHANISM OF PROTON TRANSFERS

The path of the transported proton across the width of the protein, inserted in the lipid bilayer, is in five non-consecutive segments that add up to the reactions of a single photocycle. If one could keep track of the proton, however, it would be evident that the full photocycle consists of not one but two cyclic reactions. The source of the transported proton is the retinal Schiff base, but it takes two cycles to release it to the medium. In the first cycle, the Schiff base proton replaces the proton released to the extracellular surface, and in the second cycle it will be the one released. The Schiff base proton itself is replaced in two steps also. In the first cycle, the protonation is internal and from Asp-96. In this cycle Asp-96 is the group reprotonated from the medium. It is only in the second cycle that the proton from the medium arrives to the Schiff base. After two cycles, therefore, all of the original protons in the pathway are replaced by protons from the medium.

While this schematic representation of the transport is clear and well-supported by experiments, the way the individual proton transfers occur is not at all clear. This is because the geometry of proton donors and acceptors and hydrogen-bonded water in the structures of several of the relevant intermediate states are not yet known, or not yet known at adequate resolution to decide the critical questions.

4.1 Deprotonation of the Schiff base

In the BR state the retinal is all-trans, and the proton donor Schiff base and proton acceptor Asp-85 are within a few Å from one another, bridged by water 402. In the L state the retinal is 13-cis,15-anti. When the retinal is in solution, the C-NH=C segment in this configuration is rotated 180 degrees, and orients the N-H bond in the opposite direction from the all-trans. The crystallographic structure indicates that such reorientation of the C-N=C retinal segment will have occurred after deprotonation of the Schiff base, in the M state (Luecke et al. 1999b, 2000). Given the steric and electrostatic constraints of the retinal binding site, however, it is not clear if this rotation occurs already in the L intermediate. In one suggested model, the electrostatic interaction between the positively charged Schiff base and the anionic Asp-85 will maintain the original geometry (Herzfeld and Tounge, 2000). If the N-H bond continues to point toward the extracellular side, the isomerization, that is a rotation around the C₁₃-C₁₄ double bond, will distort either the retinal chain or the Lys-216 side-chain, or more likely both. This will make the L state unstable. Relaxation of the retinal chain and/or the Lys-216 side-chain would be allowed by proton transfer from the Schiff base to Asp-85, which makes both groups electrically neutral and eliminates their electrostatic attraction. If water 402 is still present in L, it would provide the hydrogen-bond for the proton transfer. If it is absent, as in the published structures of K and L, proton transfer from the Schiff base to Asp-85 would have to be direct.

Alternatively, in the L state the N-H bond could point already toward the cytoplasmic side. The retinal would be more relaxed than in the first model, but this would be an unstable arrangement also because placing the N-H dipole into a rather hydrophobic environment has a high-energy cost. Now, water 402, highly polarized by the two anionic aspartates, Asp-85 and Asp-212, would dissociate (Luecke, 2000). The anionic state of Asp-212 being stabilized by strong hydrogen-bonds to the bulky side-chains of Tyr-185 and Tyr-57, the proton would pass to Asp-85, while the hydroxyl ion could move across the retinal to receive the proton of the Schiff base from the cytoplasmic side. This hypothetical mechanism amounts to hydroxyl ion, rather than proton, translocation at the critical step in the transport cycle. It is analogous to how chloride transport in the similar protein, halorhodopsin (Oesterhelt, 1995), and the D85T (Sasaki et al. 1995) and D85S mutants of bacteriorhodopsin might occur.

Is bacteriorhodopsin a proton pump or a hydroxyl ion pump? The answer to this interesting question awaits a high-resolution structure for the Schiff base region in the L state.

4.2 Reprotonation of the Schiff base

Reprotonation of the Schiff base, that produces the N state, is from Asp-96 on the cytoplasmic side. There are two issues to consider in this process. First, before illumination the pK_a of Asp-96 is too high (> 11) for this residue to be a proton donor. This pK_a will have been lowered before the M₂ to N reaction can occur, and the question is how?

Second, there is no hydrogen-bonded chain between Asp-96 and the Schiff base. This distance of about 10 Å must be bridged during the M to N reaction to conduct the proton to the Schiff base. A chain of water molecules are the most likely candidates for this. If so, why and how does water enter this region?

In the M_2 state, measurements with the D96N mutant have shown that the pK_a of the Schiff base is about 8.3 (Brown and Lanyi, 1996). The establishment of the approximately 1:5 protonation equilibrium between the Schiff base and Asp-96 in the M_2 to N reaction indicates that at this time the pK_a of Asp-96 must be decreased to about 7. This appears to be the result mainly of a large-scale protein conformation change (Subramaniam et al. 1993; Sass et al. 1997; Kamikubo et al. 1997) whose main component is the outward tilt of the cytoplasmic end of helix F, and other, less-understood changes at helices B and G. The evidence for this structural change consists of 3 Å resolution difference projection maps between photointermediates and the initial state, 3.2 Å resolution three-dimensional models for the N state of the F219L mutant, with long-living N (Vonck, 2000), and for a mutant with three amino acid replacements that at lower resolution and in projection resembles M or N (Subramaniam and Henderson, 2000). Another idea of the magnitude of the displacements involved is given by changes in spin-spin interaction between labels at engineered cysteines at specific locations. Thus, the distance between the label on the EF interhelical loop and labels on either the AB or the CD loop increases by several Å (Thorgeirsson et al. 1994).

The cause of these large-scale conformational changes can be traced back to the relaxation of the retinal chain after deprotonation of the Schiff base. In the “early” M state (that corresponds approximately to the M that accumulates in the illuminated E204Q mutant where proton release is blocked), the retinal assumes a less bent shape than in the “late” M of the D96N mutant (Luecke et al. 2000). This means that the angle tended by the $C_{12}-C_{13}=C_{14}$ bonds is greater than in the solution structure of retinal, and the 13-methyl group is less displaced toward the cytoplasmic side. As the 13-methyl group moves upward, it pushes against the indole ring of Trp-182, which breaks its hydrogen-bond to water 501 and thereby loses its connection to Ala-215. Helices F and G are therefore disconnected, and the ensuing movements of Trp-182 and Lys-216 cause repacking of the side-chains between the two helices. This, and the distortion of the π -bulge at Ala-215, which communicates via the main-chain of helix G and water 502 to Thr-46, moves Asp-96 and Thr-46 apart sufficiently for a new water molecule to insert between them. With an additional water molecule, the four buried waters in the cytoplasmic region, 501-504, form a hydrogen-bonded network that extends for Asp-96 toward the Schiff base but does not reach it (Luecke et al. 2000).

These structural changes help to explain how the pK_a of Asp-96 is modulated. Because the OH of Thr-46 is the hydrogen-bond donor to the C=O of Phe-42, in the BR state it must be the hydrogen-bond acceptor to the COOH of Asp-96. Maintaining the hydrogen-bond therefore requires that Asp-96 be protonated. The hydrogen-bond and the low mean dielectric constant of its hydrophobic environment, elevate the pK_a of Asp-96 to its unusually high value. Both conditions will have changed in the M state. The structural changes provide also a strong hint about the proton transfer pathway. Al-

though incomplete, the three-dimensional network of hydrogen-bonded water in M needs the addition of 2-3 water molecules to reach the Schiff base. Presumably, this is what occurs during the M to N photocycle reaction, and must be the rate-limiting step.

4.3 Reprotonation of Asp-96

The crystallographic structure of the D96G/F171C/F219L triple mutant, determined at 3.2 Å resolution, contains features surmised already from projection maps of the M and N intermediates (Subramaniam and Henderson, 2000). The structure contains not only the generally observed tilt in helix F, but also the opening of a channel at the cytoplasmic surface, through which protons were suggested to pass. This conformation is characterized by shifts of helical positions that could allow the passage of protons from the surface to Asp-96 and from Asp-96 to the Schiff base. From this structure and the projection maps of intermediate states (or mixtures of intermediate states) in other mutants, the argument was made that there is a single, altered conformation that describes the photointermediates after M₁ but before O. However, one can argue also that in such a single protein conformation Asp-96 would have to communicate with the Schiff base and the cytoplasmic surface at the same time. Because these proton transfers occur on similar time-scales (a few msec) in the photocycle, and the reprotonation of the Schiff base is pH independent, the opening of a pathway between Asp-96 and the Schiff base must precede the opening of a pathway between Asp-96 and the surface. If this is so, a two-step conformational change is required.

In a large number of single-site mutants in the region between Asp-96 and the cytoplasmic surface the decay of the N state is greatly slowed. Protonation of Asp-96 now becomes the rate-limiting step to completing the photocycle, and argues that rapid reisomerization of the retinal to all-trans requires that Asp-96 be protonated. This is consistent with other lines of evidence. Counter-intuitively, however, replacement of hydrophobic side-chains with smaller or more hydrophilic ones slowed rather than enhanced the rate of protonation of Asp-96 (Dioumaev, Brown, Needleman and Lanyi, in preparation). It appeared that a proton transfer pathway from the surface to Asp-96 is not a matter of creating simple steric access, but a more subtle structural rearrangement that is disrupted by the mutations tested. In a general way, this idea is supported by the crystallographic structure of the D85S mutant, determined to 2.25 Å resolution, as follows.

The D85X mutants (where X is N, A, T, or S, and probably anything but an Asp or Glu) are pH dependent mixtures of stable states with different chromophore absorption bands, which resemble the O state (blue, at low pH), the N state (purple, at intermediate pH), and the M state (yellow, at high pH). The resemblance has specific molecular rationales: residue 85 is uncharged in all three species, Asp-96 is protonated in the blue but not the purple and yellow species, the Schiff base is protonated in the blue and purple but not the yellow species, and the retinal is all-trans (actually a mixture of all-trans and 13-cis,15-syn) in the blue species, and 13-cis,15-anti in the purple species (and maybe also in the yellow species). These features are mostly in accordance with those of the O, N, and M intermediates (Turner et al. 1993; Dioumaev et al. 1998), although in

the D85X mutants the three states are produced without illumination, and their equilibrium is dependent on pH instead, from the protonation of Asp-96 and the Schiff base. The three states of the chromophore have strong consequences on protein conformation. The x-ray diffraction of the yellow species of D85N is virtually identical with that of a genuine M intermediate (Kataoka et al. 1994). The infrared spectrum of the photoproduct of the purple species contains the large positive/negative pair of amide bands characteristic of the N intermediate (Dioumaev et al. 1998). For these reasons, the structural differences observed between the third, blue species of D85S and wild type bacteriorhodopsin were suggested to speak to the structure of the O intermediate. D85S exhibits large-scale conformational differences from both unilluminated bacteriorhodopsin and the M or N states (Rouhani-Manshadi et al, 2001). The tilt of helix F is absent, but the extracellular end of helix E swivels outward (pivoting at its middle), as do the extracellular ends of helices A, B and D. As expected, the region near the cytoplasmic surface is disrupted by displacement of helix E. It becomes more hydrated, with three new water molecules located between the surface and Asp-96. They could be the remains of the proton transfer chain that allowed protonation of Asp-96. On the extracellular side, additional water molecules observed which might establish the pathway of the proton from Asp-85 to the proton release site during the decay of the O state.

4.4 Deprotonation of Asp-85

In the last step of the photocycle Asp-85 loses its proton to the vacant extracellular proton release site (which had dissociated during the rise of the M state). The twist evident from FTIR spectra of the all-trans retinal chain in O relaxes, completing the recovery of the initial state. The limiting step appears to be the deprotonation of Asp-85, a consequence of the recovery of its initial very low pK_a (about 2.5). Indeed, there is good correlation when mutants in this region are compared with regard to the rate of the deprotonation of Asp-85 in a pH jump experiment in the dark (from pH 2 to 6) and the rate of the decay of O in the photocycle (Richter et al. 1996a). While these reactions are obviously driven by the incompatibility of the reisomerized all-trans retinal and the still protonated Asp-85, how and why they occur is not clear. The only structural clue is from the x-ray diffraction data for the D85S mutant. As expected from its proposed resemblance to the O state, the extracellular region of D85S is considerably altered. The outward tilt of helices A, C and E appear to open a putative proton channel between Asp-85 and the Glu-194/Glu-204 pair. Two additional water molecules are hydrogen-bonded to the two NH₂ groups of Arg-82, and might play a role in the proton transfer from the aspartic acid to the proton release site during decay of the O state.

5. NATURE OF THE PROTON TRANSFER SWITCH

The minimal functional requirement of any ion pump is the existence of an ion binding site that becomes alternatively accessible to the two membrane sides, and a driving reaction that causes the unidirectional cycling of the pump through the states with differing accessibilities. The mechanism by which the access and its change, the "switch," are accomplished is the central question in understanding the transport proc-

ess. In principle, this mechanism may use switches of two kinds: (a) a switch that utilizes suitable donor and acceptor sites, to either side of the central ion binding site, which undergo appropriately timed affinity changes for the transported ion, and (b) a switch that opens and closes the ion transfer pathways to either side of the central ion binding site. Alternatives a) and b) represent extreme examples, and are not mutually exclusive. In case (a) accessibility to either side must exist throughout, and conversely, in case (b) affinity changes, or even acceptor or donor sites, are not necessary.

This kind of thinking underlies, explicitly in many cases and implicitly in others, how a very large amount of experimentation with bacteriorhodopsin and many complex results are viewed and interpreted. The most interesting approach to the question of the switch is to simplify the protein by replacing the proton acceptor, Asp-85, alone or together with the proton donor, Asp-96, with asparagine, and examine the photocycle properties and evidence of any residual transport. The implications of the results are far-reaching.

The phenotype of Asp-85 mutants is distinctive. Lacking the strong counter-ion that the anionic Asp-85 provides, the pK_a of the protonated Schiff base in D85N is greatly lowered. Above pH 9, the Schiff base is unprotonated even without illumination, and the chromophore is yellow. The overall structure of the protein now resembles the structure of M (Kataoka et al. 1994). Surprisingly, photoexcitation of this M-like species (with blue light rather than yellow because of its shifted absorption maximum), was found to result in proton transport, and in the same direction as the wild type pump (Tittor et al. 1994). The protons transported per cycle was much less than in the wild-type, but it was transport nonetheless. This suggested there are connectivity changes during the reaction cycle dependent only on the retinal Schiff base. Even more unexpected was the observation of these authors that a two-photon reaction with both blue and yellow lights resulted in transport in the direction opposite from the wild type. How do these kinds of transport occur, and what is their relevance for understanding transport in the wild type?

There appeared to be two alternative explanations. In the "IST" model (Haupt et al. 1997), both the change in the direction of proton transfer pathways and the proton transfers themselves are postulated to be direct consequences of the isomerization of the retinal (I^* photoisomerization, I thermal isomerization). The switch (S) and the transfer (T) and their reversals that regenerate the initial state are thus viewed as distinct processes, independent of one another. Depending on the mutant and the illumination regime, there is kinetic competition between the switch event and the proton transfer event. Which occurs first determines whether or not there is transport. It was postulated that in the wild type the first transfer is before the switch ($I^*/T/S/T/I/S$), so deprotonation of the Schiff base is to the extracellular side but its reprotonation in the second transfer is from the cytoplasmic side. In mutants of Asp-85 with unprotonated Schiff base the switch comes before the first transfer ($I^*/S/T/I/S/T$), so reprotonation is again from the cytoplasmic side, which allows reisomerization and the second switch which results in proton release to the extracellular side. In this way, the transport capabilities

of many, or perhaps all, complex mutants under one-photon and two-photon illumination regimes can be explained formally by various sequences for I, S, and T.

In the “local-access” model (Brown et al. 1998a,b) each photocycle step is the consequence of the one preceding it. Thus, unlike in the IST model, there can be no kinetic competition between S and T. Further, this model recognizes that it might not be possible to assign the switch, S, to a single step, separate from T. For example, if the proton access were to remain open in either direction (as is the case under some conditions), a protonation equilibrium would develop among the Schiff base, Asp-85, and Asp-96. If progress toward recovery of the initial state required also that Asp-96 be unprotonated, and it were connected to a unidirectional reaction (i.e., decay of the O state), the directionality of the transport would be established by the shift of the equilibrium away from deprotonation of Asp-85 and toward deprotonation of Asp-96. Which step is the switch now? In this scenario, the distinction between S and T is blurred.

The basis for the local-access model is a large amount of experimental data on the D85N/D96N mutant (Brown et al. 1998a). The results indicate that, in this mutant with residue 85 uncharged, the proton accessibility at the Schiff base depends on the isomeric state of the retinal, but not in the sense of the intuitive flip/flop between two directions. When the retinal is all-trans, access of the Schiff base proton is in the extracellular direction. When the retinal is 13-cis,15-anti and residue 85 is uncharged (because it is an asparagine in the mutant, or it is an aspartic acid that becomes protonated in the photocycle of the wild type), a conformational equilibrium develops in which both directions are, to some extent, accessible. The unprotonated Schiff base in the mutant will receive a proton from the proton channel of higher conductivity, which is in the cytoplasmic direction. Reprotonation of the Schiff base allows the thermal reisomerization of the retinal, which returns the local access to its initial position, i.e., toward the extracellular side. Deprotonation of the Schiff base will be therefore in that direction, yielding net transport. Under these conditions (and different from the wild type mechanism), there is no modulation of the proton conductivities of the two channels, which act passively. Hence the term, “local-access.”

The elements of this model are rearranged when applied to the photocycle of the wild type protein, but the principle remains the same. In the wild type also, this model gives a straight-forward mechanistic explanation for the switch. Initial access is in the extracellular direction, because the retinal is all-trans and Asp-85 is anionic. The proton transfer from Schiff base to Asp-85 (either directly or via dissociation of water 402) is the consequence of the photoisomerization. Release of a proton to the extracellular surface raises the pK_a of Asp-85, through the coupling of the pK_a of release site to the pK_a of this residue. This closes the extracellular proton channel, and reprotonation is preferentially from the cytoplasmic side. Thus, the change of proton transfer pathway from extracellular to cytoplasmic is the direct consequence of the protonation of Asp-85.

What happens at acid pH, which hinders proton release? The pK_a of Asp-85 is not raised, and the protonation equilibrium between the Schiff base and Asp-85 will persist (Zimányi et al. 1992; Dickopf and Heyn, 1997; Brown et al. 1998b). Transport requires

that proton access from the cytoplasmic side is established also. The model thus predicts that with time these groups will come to an additional equilibrium, with Asp-96. The last reaction of the photocycle, unidirectional because of a large loss of free energy, will shift the chain of equilibria toward the last species, the O state, thereby depleting the intermediate states, one by one. The photocycle will come to full completion, in spite of its reversible reactions, because the last step is irreversible.

This model could be tested with a two-flash experiment, in which M is produced by a green flash and then depleted by a second, blue flash (Brown et al. 1998b). It showed that after the blue flash the ratio of L and M recovers. L is depleted and M is repopulated, and L/M ratio is reestablished. This observation confirmed that the L and M states are in equilibrium. The re-equilibration was pH dependent with the same pK_a as proton release, as expected from the postulated mechanism. Because the Schiff base was reprotonated from the cytoplasmic side, these experiments provided the evidence sought that at acid pH at least, protons can pass from both Asp-85 and Asp-96 to the Schiff base.

6. REFERENCES

- Althaus, T., Einfeld, W., Lohrmann, R., and Stockburger, M. 1995. Application of Raman spectroscopy to retinal proteins. *Israel J.Chem.* 35:227-252.
- Balashov, S. P., Imasheva, E. S., Govindjee, R., and Ebrey, T. G. 1996. Titration of aspartate-85 in bacteriorhodopsin: What it says about chromophore isomerization and proton release. *Biophys.J.* 70: 473-481.
- Balashov, S. P. and Ebrey, T. G. 2001. Trapping and spectroscopic identification of the photointermediates of bacteriorhodopsin at low temperatures. *Photochem. Photobiol.* 73: 453-462.
- Belrhali, H., Nollert, P., Royant, A., Menzel, C., Rosenbusch, J. P., Landau, E. M., Pebay-Peyroula, E. Protein, lipid and water organization in bacteriorhodopsin crystals: a molecular view of the purple membrane at 1.9 Å resolution. *Structure.Fold.Des* 7:909-917, 1999.
- Braiman, M. S., Bousché, O., and Rothschild, K. J. 1991. Protein dynamics in the bacteriorhodopsin photocycle: Submillisecond Fourier transform infrared spectra of the L, M, and N photointermediates. *Proc.Natl.Acad.Sci.U.S.A.* 88:2388-2392.
- Brown, L. S. and Lanyi, J. K. 1996. Determination of the transiently lowered pK_a of the retinal Schiff base during the photocycle of bacteriorhodopsin. *Proc.Natl.Acad.Sci.U.S.A.* 93:1731-1734.
- Brown, L. S., Dioumaev, A. K., Needleman, R. and Lanyi, J. K. 1998a. Local-access model for proton transfer in bacteriorhodopsin. *Biochemistry* 37: 3982-3993.

Brown, L. S., Dioumaev, A. K., Needleman, R. and Lanyi, J. K. 1998b. Connectivity of the retinal Schiff-base to asp85 and asp96 during the bacteriorhodopsin photocycle: The local-access model. *Biophys.J.* 75: 1455-1465.

Brown, L. S., Needleman, R., and Lanyi, J. K. 1999. Functional roles of aspartic acid residues at the cytoplasmic surface of bacteriorhodopsin. *Biochemistry* 38: 6855-6861.

Cao, Y., Váró, G., Chang, M., Ni, B., Needleman, R., and Lanyi, J. K. 1991. Water is required for proton transfer from aspartate 96 to the bacteriorhodopsin Schiff base. *Biochemistry* 30:10972-10979.

Chernavskii, D. S., Chizhov, I. V., Lozier, R. H., Murina, T. M., Prokhorov, A. M., and Zubov, B. V. 1989. Kinetic model of bacteriorhodopsin photocycle: pathway from M state to bR. *Photochem.Photobiol.* 49:649-653.

Delaney, J. K. and Schweiger, U., and Subramaniam, S. 1995. Molecular mechanism of protein-retinal coupling in bacteriorhodopsin. *Proc.Natl.Acad.Sci.U.S.A.* 92: 11120-11124.

Dencher, N. A. and Heyn, M.P. 1979. Bacteriorhodopsin monomers pump protons. *FEBS Lett.* 108: 307-10.

Dickopf, S. and Heyn, M. P. 1997. Evidence for the first phase of the reprotonation switch of bacteriorhodopsin from time-resolved photovoltage and flash photolysis experiments on the photoreversal of the M-intermediate. *Biophys.J.* 73: 3171-3181.

Dioumaev, A. K., Brown, L. S., Needleman, R., and Lanyi, J. K. 1998. Partitioning of free energy gain between the photoisomerized retinal and the protein in bacteriorhodopsin. *Biochemistry* 37: 9889-9893.

Druckmann, S., Friedman, N., Lanyi, J. K., Needleman, R., Ottolenghi, M. and Sheves, M. 1992. The Back Photoreaction of the M Intermediate in the Photocycle of Bacteriorhodopsin: Mechanism and Evidence for two M Species. *Photochem. PhotoBiol.* 56: 1041-1047.

Ebrey, T. G. 1993. Light energy transduction in bacteriorhodopsin. In: *Thermodynamics of membranes, receptors and channels*, ed. Jackson, M., pp. 353-387, CRC Press, New York.

Edman, K., Nollert, P., Royant, A., Belrhali, H., Pebay-Peyroula, E., Hajdu, J., Neutze, R. and Landau, E. M. 1999. High-resolution X-ray structure of an early intermediate in the bacteriorhodopsin photocycle. *Nature* 401: 822-826.

- Grigorieff, N., Ceska, T. A., Downing K. H., Baldwin, J. M. and Henderson, R. 1996. Electron-crystallographic refinement of the structure of bacteriorhodopsin. *J.Mol.Biol.* 259: 393-421.
- Haupts, U., Tittor, J., Bamberg, E., and Oesterhelt, D. 1997. General concept for ion translocation by halobacterial retinal proteins: The isomerization/switch/ transfer (IST) model. *Biochemistry* 36: 2-7.
- Haupts, U., Tittor, J., and Oesterhelt, D. 1999. Closing in on bacteriorhodopsin: progress in understanding the molecule. *Annu.Rev.Biophys.Biomol.Struct.* 28: 367-399
- Heberle, J. and Dencher, N. A. 1992. Surface-bound optical probes monitor proton translocation and surface potential changes during the bacteriorhodopsin photocycle. *Proc.Natl.Acad.Sci.U.S.A.* 89:5996-6000.
- Heberle, J., Riesle, J., Thiedemann, G., Oesterhelt, D., and Dencher, N. A. 1994. Proton migration along the membrane surface and retarded surface to bulk transfer. *Nature* 370: 379-382.
- Henderson R., and Unwin P. N. 1975. Three-dimensional model of purple membrane obtained by electron microscopy. *Nature* 257: 28-32.
- Henderson, R., Baldwin, J. M., Ceska, T. A., Zemlin, F., Beckmann, E. and Downing, K. H. 1990. Model for the structure of bacteriorhodopsin based on high-resolution electron cryo-microscopy. *J.Mol.Biol.* 213: 899-929.
- Herzfeld, J. and Tounge, B. 2000. NMR probes of vectoriality in the proton-motive photocycle of bacteriorhodopsin: evidence for an "electrostatic steering" mechanism. *Biochim. Biophys. Acta* 1460: 95-105.
- Kamikubo, H., Oka, T., Imamoto, Y., Tokunaga, F., Lanyi, J. K., and Kataoka, M. 1997. The last phase of the reprotonation switch in bacteriorhodopsin: the transition between the M-type and the N-type protein conformation depends on hydration. *Biochemistry* 36:12282-12287.
- Kataoka, M., Kamikubo, H., Tokunaga, F., Brown, L. S., Yamazaki, Y., Maeda, A., Sheves, M., Needleman, R., and Lanyi, J. K. 1994. Energy coupling in an ion pump: the reprotonation switch of bacteriorhodopsin. *J.Mol.Biol.* 243: 621-638.
- Kimura, Y., Vassilyev, D. G., Miyazawa, A., Kidera, A., Matsushima, M., Mitsuoka, K., Murata, K., Hirai, T., and Fujiyoshi, Y. 1997. Membrane surface structure and proton pathway of bacteriorhodopsin analyzed by electron crystallography. *Nature* 389:206-211.

- Lanyi, J. K. 2000a. Molecular Mechanism of Ion Transport in Bacteriorhodopsin: Insights from Crystallographic, Spectroscopic and Mutational Studies. *J. Physical Chemistry B* 104: 11441-11448.
- Lanyi, J. K. (ed.) 2000b. Bacteriorhodopsin: a special issue of *Biochim. Biophys. Acta*, 1460: 1-239.
- Lanyi, J. K. 1993. Proton translocation mechanism and energetics in the light-driven pump bacteriorhodopsin. *Biochim. Biophys. Acta* 1183: 241-261.
- Lanyi, J. K. and Váró, G. 1995. The photocycles of bacteriorhodopsin. *Israel J. Chem.* 35:365-386.
- Luecke, H. 2000. Atomic resolution structures of bacteriorhodopsin photocycle intermediates: the role of discrete water molecules in the function of this light-driven ion pump. *Biochim Biophys Acta* 1460: 133-56.
- Luecke, H. Richter, H. T. and Lanyi, J. K. 1998. Proton Transfer Pathways in Bacteriorhodopsin at 2.3 Angstrom Resolution. *Science* 280: 1934-1937.
- Luecke, H., Schobert, B., Richter, H. T., Cartailler, J. P. and Lanyi, J. K. 1999a. Structure of bacteriorhodopsin at 1.55 Å resolution. *J. Mol. Biol.* 291:899-911.
- Luecke H., Schobert, B., Richter, H. -T., Cartailler, J. -P, and Lanyi, J. K. 1999b. Structural Changes in the M Photointermediate of Bacteriorhodopsin at 2 Angstrom Resolution. *Science* 286: 255-260.
- Luecke, H., Schobert, B., Cartailler, J.-P., Richter, H. -T., Rosengarth, A., Needleman, R. and Lanyi, J. K. 2000. Coupling Photoisomerization of Retinal to Directional Transport in Bacteriorhodopsin. *J. Mol. Biol.* 300: 1237-1255, 2000.
- Maeda, A. 1995. Application of FTIR spectroscopy to the structural study on the function of bacteriorhodopsin. *Israel J. Chem.* 35:387-400, 1995.
- Maeda, A., Kandori, H., Yamazaki, Y., Nishimura, S., Hatanaka, M., Chon, Y. S., Sasaki, J., Needleman, R., and Lanyi, J. K. 1997. Intramembrane signaling mediated by hydrogen-bonding of water and carboxyl groups in bacteriorhodopsin and rhodopsin. *J. Biochem. (Tokyo)* 121:399-406.
- Mathies, R. A., Lin, S. W., Ames, J. B., and Pollard, W. T. 1991. From femtoseconds to biology: Mechanism of bacteriorhodopsin's light-driven proton pump. *Annu. Rev. Biophys. Biophys. Chem.* 20: 491-518.
- Oesterhelt, D. 1995. Structure and function in halorhodopsin. *Israel J. Chem.* 35:475-494.

- Oesterhelt, D., Tittor, J., and Bamberg, E. A unifying concept for ion translocation by retinal proteins. *J.Bioenerg.Biomembr.* 24: 181-191, 1992.
- Pfeiffer, M., Rink, T., Gerwert, K., Oesterhelt, D., and Steinhoff, H. J. 1999. Site-directed spin-labeling reveals the orientation of the amino acid side-chains in the E-F loop of bacteriorhodopsin. *J.Mol.Biol.* 287: 163-171.
- Rammelsberg, R., Huhn, G., Lübben, M., and Gerwert, K. 1998. Bacteriorhodopsin's intramolecular proton-release pathway consists of a hydrogen-bonded network. *Biochemistry* 37: 5001-5009.
- Richter, H. T., Needleman, R., Kandori, H., Maeda, A., and Lanyi, J. K. 1996a. Relationship of retinal configuration and internal proton transfer at the end of the bacteriorhodopsin photocycle. *Biochemistry* 35: 15461-15466.
- Richter, H. T., Brown, L. S., Needleman, R., and Lanyi, J. K. 1996b. A linkage of the pK_a's of asp-85 and glu-204 forms part of the reprotonation switch of bacteriorhodopsin. *Biochemistry* 35: 4054-4062.
- Riesle, J., Oesterhelt, D., Dencher, N. A., and Heberle, J. 1996. D38 is an essential part of the proton translocation pathway in bacteriorhodopsin. *Biochemistry* 35: 6635-6643.
- Rouhani-Manshadi, S., Cartailier, J-P., Faciotti, M. T., Walian, P., Needleman, R., Lanyi, J.K., Glaeser, R.M., Luecke, H. (2001) *J.Mol.Biol.* (in press).
- Royant, A., Edman K., Ursby T., Pebay-Peyroula E., Landau E. M. and Neutze R. 2000. Helix deformation is coupled to vectorial proton transport in the photocycle of bacteriorhodopsin. *Nature*, 406:645-648.
- Rummel, G., Hardmeyer, A., Widmer, C., Chiu, M. L., Nollert, P., Locher, K. P., Pedruzzi, I. I., Landau, E. M. and Rosenbusch, J. P. 1998. Lipidic cubic phases: new matrices for the three-dimensional crystallization of membrane proteins. *J Struct Biol.* 121: 82-91.
- Sasaki, J., Brown, L. S., Chon, Y. -S., Kandori, H., Maeda, A., Needleman, R., and Lanyi, J. K. 1995. Conversion of bacteriorhodopsin into a chloride ion pump. *Science* 269: 73-75.
- Sass, H. J., Schachowa, I. W., Rapp, G., Koch, M. H. J., Oesterhelt, D., Dencher, N. A., and Büldt, G. 1997. The tertiary structural changes in bacteriorhodopsin occur between M states; X-ray diffraction and Fourier transform infrared spectroscopy. *EMBO J.* 16:1484-1491.
- Sass, H. J., Buldt, G., Gessenich, R., Hehn, D., Neff, D., Schlesinger, R., Berendzen, J. and Ormos, P. 2000. Structural alterations for proton translocation in the M state of wild-type bacteriorhodopsin. *Nature* 2000, 406:649-653.

- Scherrer, P., Alexiev, U., Marti, T., Khorana, H. G., and Heyn, M. P. 1994. Covalently bound pH-indicator dyes at selected extracellular or cytoplasmic sites in bacteriorhodopsin. 1. Proton migration along the surface of bacteriorhodopsin micelles and its delayed transfer from surface to bulk. *Biochemistry* 33:13684-13692.
- Steinhoff, H. -J., Mollaaghababa, R., Altenbach, C., Hideg, K., Krebs, M., Khorana, H. G., and Hubbell, W. L. 1994. Time-resolved detection of structural changes during the photocycle of spin-labeled bacteriorhodopsin. *Science* 266: 105-107.
- Subramaniam, S., Gerstein, M., Oesterhelt, D., and Henderson, R. 1993. Electron diffraction analysis of structural changes in the photocycle of bacteriorhodopsin. *EMBO J.* 12: 1-8.
- Subramaniam, S. and Henderson, R. 2000. Molecular mechanism of vectorial proton translocation by bacteriorhodopsin. *Nature*, 406: 653-657.
- Thorgeirsson, T. E., Xiao, W., Brown, L. S., Needleman, R., Lanyi, J. K., and Shin, Y.-K. 1997. Opening of the cytoplasmic proton channel in bacteriorhodopsin. *J.Mol.Biol.* 273: 951-957.
- Tittor, J., Schweiger, U., Oesterhelt, D., and Bamberg, E. 1994. Inversion of proton translocation in bacteriorhodopsin mutants D85N, D85T and D85,D96N. *Biophys.J.* 67: 1682-1690.
- Turner, G. J., Miercke, L. J. W., Thorgeirsson, T. E., Kliger, D. S., Betlach, M. C., and Stroud, R. M. 1993. Bacteriorhodopsin D85N: Three spectroscopic species in equilibrium. *Biochemistry* 32: 1332-1337.
- Váró, G. and Lanyi, J. K. 1991. Thermodynamics and energy coupling in the bacteriorhodopsin photocycle. *Biochemistry* 30: 5016-5022.
- Vonck, J. 2000. Structure of the bacteriorhodopsin mutant F219L N intermediate revealed by electron crystallography. *EMBO J*19:2152-60.
- Weidlich, O., Schalt, B., Friedman, N., Sheves, M., Lanyi, J. K., Brown, L. S., and Siebert, F. 1996. Steric interaction between the 9-methyl group of the retinal and tryptophan 182 controls 13-cis to all-trans isomerization and proton uptake in the bacteriorhodopsin photocycle. *Biochemistry* 35: 10807-10814.
- Yamazaki, Y., Sasaki, J., Hatanaka, M., Maeda, A., Kandori, H., Needleman, R., Shinada, T., Yoshihara, K., Brown, L. S., and Lanyi, J. K. 1995. Interaction of tryptophan182 with the 9-methyl group of the retinal in the L intermediate of bacteriorhodopsin. *Biochemistry* 34: 577-582.

Zheng, L. and Herzfeld, J. 1992. NMR studies of retinal proteins. *J.Bioenerg. Biomembr.* 24: 139-146.

Zimányi, L., Váró, G., Chang, M., Ni, B., Needleman, R., and Lanyi, J. K. 1992a. Pathways of proton release in the bacteriorhodopsin photocycle. *Biochemistry* 31: 8535-8543.

Zimányi, L. and Lanyi, J. K. 1992b. The Two Consecutive M Substates in the Photocycle of Bacteriorhodopsin are Affected Specifically by the D85N and D96N Residue Replacements. *Photochem. PhotoBiol.* 56: 1049-1055.